# We are IntechOpen, the world's leading publisher of Open Access books Built by scientists, for scientists

6,900
Open access books available

185,000
International authors and editors

200M
Downloads

Our authors are among the

154
Countries delivered to

TOP 1%
most cited scientists

12.2%
Contributors from top 500 universities




WEB OF SCIENCE™

Selection of our books indexed in the Book Citation Index in Web of Science™ Core Collection (BKCI)

## Interested in publishing with us?
## Contact book.department@intechopen.com

Numbers displayed above are based on latest data collected.
For more information visit www.intechopen.com



Chapter

# Third-Order Nonlinear Optical Properties of Quantum Dots

*Khalil Ebrahim Jasim*

## Abstract

Quantum dots (QDs) are semiconducting nanocrystalline particles. QDs are attractive photonic media. In this chapter, we introduce third-order nonlinear optical properties and a brief idea about the physics of QDs. Z-scan technique and theoretical analysis adopted to obtain nonlinear parameters will be discussed. Analysis of third-order nonlinear optical parameters for PbS QDs suspended in toluene with radii 2.4 and 5.0 nm under different excitation beam power level and three different wavelengths (488, 514, and 633 nm) will be detailed. Third-order optical susceptibility $\chi^{(3)}$ and optical-limiting behavior of PbS QD suspended in toluene are presented. Irrespective of their size, QDs are a good example of optical limiters with low threshold.

**Keywords:** quantum dot, semiconductor, nonlinear optics, Z-scan technique, nonlinear index of refraction, nonlinear absorption coefficient, third-order optical susceptibility, optical limiting, optical switching

## 1. Introduction

Generally speaking, quantum dots (QDs) are nanocrystalline structures that can be grown using physical or chemical methods. QDs are an essential medium for extensive range of applications in photonics. Some attention-grabbing applications of these materials include fluorescence imaging, electroluminescence, frequency up conversion lasing, stabilization of laser power fluctuations, photon microscopy, solar cells, optical signal reshaping, and nonlinear optics. QDs demonstrate a strong confinement for both electrons and holes due to size effect (quantum confinement). Therefore, nonlinear optical properties are expected to be greatly enhanced in QD media, due to flexibility of their electronic and optical properties that are controlled via choosing the precise size and concentration in the system. This chapter will discuss the physics and capacity of QDs as a nonlinear medium. Introductory idea about nonlinear optics will be outlined. Then, theoretical background of the Z-scan technique used to investigate QDs' third-order nonlinear optical properties will be detailed. As an example, characterization of lead sulfide (PbS)'s nonlinear optical properties will be presented.

## 2. Physics of quantum dots

In bulk structure of semiconductors, charge carriers (electrons and holes) have continuous distribution of energy states and their motion is not confined. However,

in quantum well (QW) structures, these charge carries are confined and their energy states are quantized in one dimension. Further confinement and quantization of energy in two dimensions is achieved in quantum wire structures where motion of charge carriers is confined and energy states are quantized in two dimensions. Confinement of electron in three dimensions and hence quantization of its energy states can be established in quantum dot structures. QDs can be treated as zero-dimensional bulk solids. QDs are nanostructured semiconductor crystalline media. In QD structure, the density of states can be represented by a delta function, as illustrated in **Figure 1a**. In this system, only discrete energy levels are allowed with a specific wave vector **k** value for each allowed energy state (**Figure 1b** and **c**).

The energy gap of a QD can be estimated as the sum of the bandgap energy, the confinement energy, and the bound exciton energy. The bandgap energy is determined by the size of the quantum dot. In strong confinement regime, the size of the QD is smaller than the exciton Bohr radius $a_{\mathrm{EBR}}$, where the energy levels split up. In this case, we have

$$a_{EBR} = \varepsilon_r \left(\frac{m}{\mu}\right) a_B \tag{1}$$

where $m$ is the mass, μ is the reduced mass, $\varepsilon_r$ is the size-dependent dielectric constant, and $a_B = 0.53 \times 10^{-10}$ m is the Bohr radius. **Table 1** shows values of $a_{\mathrm{EBR}}$ for some common semiconductors [1].

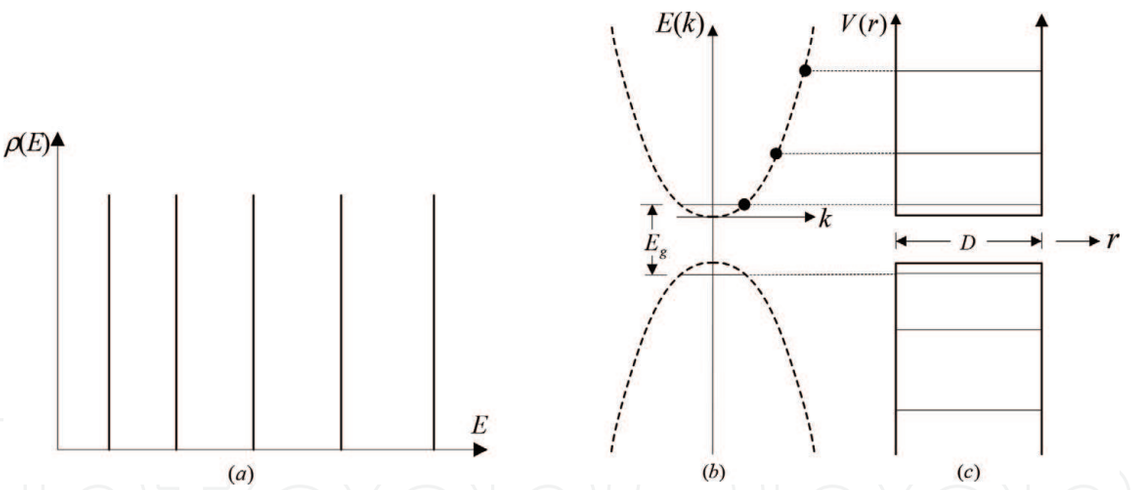



**Figure 1.**
*(a) Energy density of states in QDs is represented by delta functions; (b) due to confinement effect, the energy gap is larger than that of the bulk material; (c) allowed energy in QDs is ideally that of an infinite quantum well.*

| Semiconductor structure | Exciton Bohr radius (nm) | Bandgap energy (eV) |
|---|---|---|
| PbS | 40.0 | 0.41 |
| GaAs | 28.0 | 1.43 |
| CdTe | 15.0 | 1.50 |
| CdSe | 10.6 | 1.74 |
| ZnSe | 8.4 | 2.58 |
| CdS | 5.6 | 2.53 |

**Table 1.**
*Exciton Bohr radius and bandgap energy of some common semiconductors [1].*

The total energy released in the emission can thus be written as

$$E_{total} = E_{Bandgap} + E_{Confinment} + E_{Exciton} \tag{2}$$

where $E_{Bandgap}$ is the bulk bandgap. Hence, according to [2], the last two terms in Eq. (2) are,

$$E_{Confinment} = \frac{\eta^2\pi^2}{2R^2}\left(\frac{1}{m_e} + \frac{1}{m_h}\right) = \frac{\eta^2\pi^2}{2\mu R^2} \tag{3}$$

and

$$E_{exciton} = -\frac{1.8e^2}{2\pi\varepsilon_0\varepsilon_r R} \tag{4}$$

In the above equations, $m_n$ and $m_p$ are the electron and hole effective masses, respectively, $\varepsilon_0 = 8.8545 \times 10^{-12}$ F/m is the permittivity of free space, and $R$ is the QD radius. Other quantities are as defined above.

The above simple model shows that the energy of QDs is dominated by the quantum confinement effect (Eq. 3), where the energy varies inversely with the square of the QD's radius. **Figure 2** shows absorbance spectrum obtained using dual-beam spectrophotometer for PbS QDs with different radii (sizes); as the size of the QD decreases, its bandgap energy increases (blue shift of the excitonic peak).

It is interesting to note that QDs unlike organic dyes when excited their fluorescence is much stronger and absorbance peak is widely spaced from that of fluorescence as presented in **Figure 3**, the peak emission wavelength is bell-shaped (Gaussian) and occurs at a slightly longer wavelength than the lowest energy exciton peak (the absorption onset). This energy separation is what is referred to as the Stokes shift. Therefore, there is less overlapping between absorbance and fluorescence spectra. Moreover, the QD's bleaching and damage threshold is much more than that of organic dyes.

**Figure 4** shows fluorescence spectrum of excited PbS quantum dots suspended in toluene. As the excitation power increases, fluorescence intensity increases without any noticeable shift in the fluorescence peak.

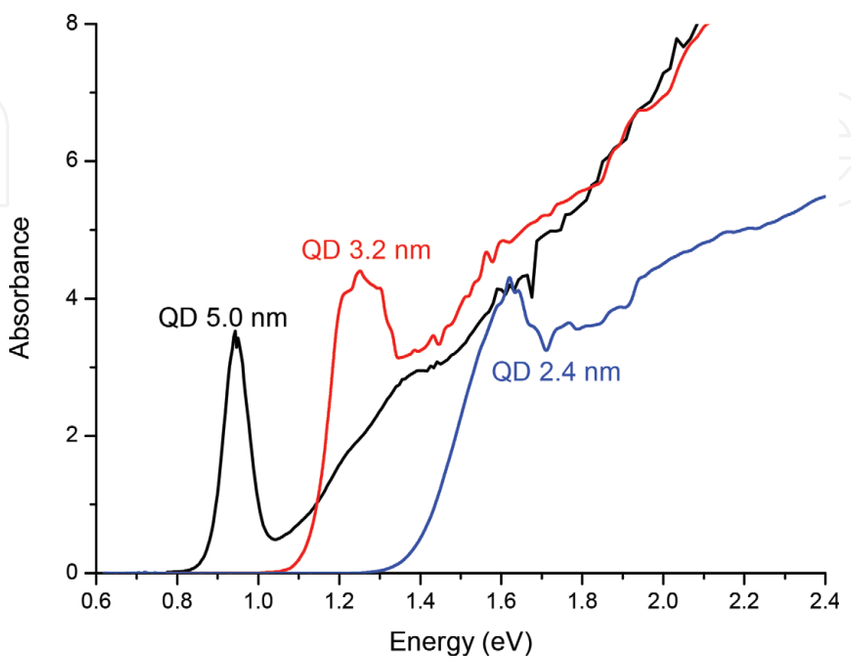



**Figure 2.**
*Energy dependence versus absorbance of PbS QDs with three different sizes.*

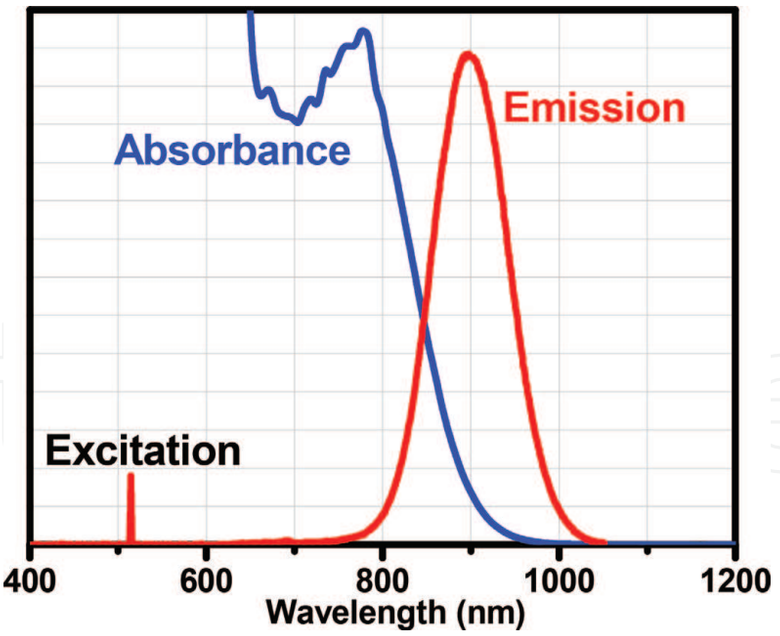



**Figure 3.**
*Absorbance and fluorescence spectra for PbS QD of size 2.4 nm.*

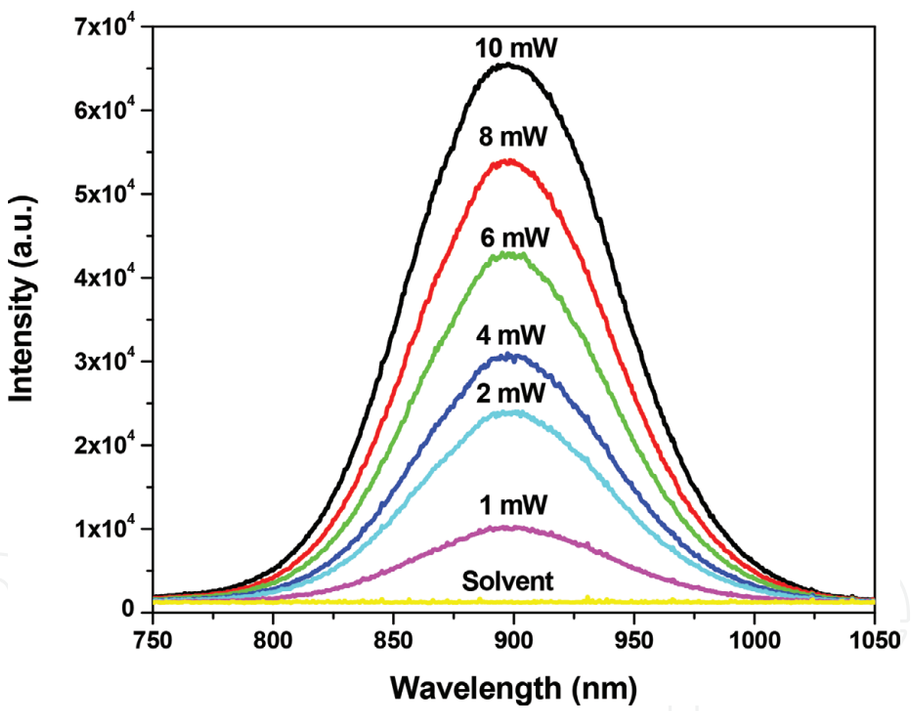



**Figure 4.**
*Fluorescence spectra for PbS QDs of size 2.4 nm excited with Ar laser of λ = 514 nm at different beam power.*

## 3. Nonlinear optics

Generally speaking, nonlinear optics is a branch in photonics concerned with studying optical properties and applications of nonlinear optical materials. Nonlinear optical media interact with electromagnetic waves in a manner different than what we get used to with ordinary materials such as glass slide or water. A linear optical material reflects, transmits, and absorbs part of a light beam incident on it without altering its nature such as color (frequency). Linear media respond to electromagnetic waves (EM) in a linear fashion. Therefore, it is a passive optical

media. On the other hand, there are materials that upon interaction with EM waves of specific intensity become active and they behave as self-focusing (positive lens) or self-defocusing (negative lens), diffracting, beam fanning, or optical limiting media. Nonlinear optical media can be used to generate new frequencies.

### 3.1 Intensity-dependent refractive index and absorption coefficient

The result of the interaction between low-intensity non-coherent light beam and high-intensity coherent light beam differs as the normal (non-coherent) light interaction shows a linear response to the electromagnetic (EM) field and the optical characteristics of the material remain unchanged because they do not rely on the light intensity and the frequency remains constant. The occurrence of superposition is possible, but the waves do not interact with each other. On the other hand, the interaction between the laser (coherent) beam and the material shows a nonlinear response to the electromagnetic field and the optical characteristics of the material such as refractive index and the speed of light do change. Superposition principle does not apply because of interaction of light with light [3, 4]. Nonlinear refraction might occur from molecular reorientation, the electronic Kerr effect, or optically induced heating of the material [5–7].

The refractive index of NLO materials can be described by the following relation [8]:

$$n(I) = n_0 + n_2 I = n_0 + \Delta n \tag{5}$$

where $n_0$ is the linear refractive index, I is the incident optical field density or intensity (irradiance), and $n_2$ is a new optical constant which is called the second-order index of refraction (nonlinear refractive index coefficient). $n_2$ is the rate when the refractive index increases with increasing optical density. The change in refractive index Δn, in Eq. (5), which is proportional to the square of the applied electric field is called optical Kerr effect. The reported order of magnitude of $n_2$ for semiconductors is from $10^{-10}$ to $10^{-2}$ cm/W. It has been found that both magnitude and sign of $n_2$ are sensitive to both the wavelength and polarization state of the exciting laser beam [8]. The total refractive index n(I) is a linear function of intensity I.

The nonlinear absorption of NLO materials can be described by the following relation:

$$\alpha\,(I) = \alpha_0 + \beta\, I \tag{6}$$

where $\alpha_0$ is the linear absorption coefficient, and β is the nonlinear absorption coefficient.

Both nonlinear index of refraction and nonlinear absorption coefficient are related to third-order optical susceptibility as given by the following relations, [9, 10]:

$$\mathrm{Re}\chi^{(3)}(esu) = \left(\frac{\varepsilon_0 c^2}{10^4 \pi}\right) n_0^2 n_2 \ \ (cm^2/W) \tag{7}$$

$$\mathrm{Im}\chi^{(3)}(esu) = \left(\frac{\varepsilon_0 c^2}{4 \times 10^2 \pi^2}\right) n_0^2 \lambda \beta \ \ (cm/W) \tag{8}$$

$$\left|\chi^{(3)}\right| = \sqrt{\left(\mathrm{Re}\chi^{(3)}\right)^2 + \left(\mathrm{Im}\chi^{(3)}\right)^2} \tag{9}$$

Here $c$ is the speed of light in vacuum ($3 \times 10^8$ m/s), $\varepsilon_0$ is the permittivity of free space ($8.854 \times 10^{-12}$ F/m), and $n_0$ is the linear index of the sample.

## 3.2 Third-order nonlinear processes

### *3.2.1 Self-phase modulation (SPM)*

Self-phase modulation (SPM) is a nonlinear optical phenomenon of light-matter interaction which has been discovered in the early days of nonlinear optics. The strong field of a laser beam (coherent waves), when propagating in a third-order nonlinear medium, interacts with the medium and induces a varying refractive index of the medium due to the optical Kerr effect. This interaction imposes a phase shift in the laser pulse, leading to a change of the pulse's frequency spectrum [3, 8]. In brief, self-phase modulation is the intensity-dependent nonlinear refractive index that modulates the optical phase ($\Delta\phi$) of the laser beam electric field which is given by the following relation:

$$\Delta\phi = 2\pi n_2 L \frac{P}{A\lambda_o} \tag{10}$$

where P is the optical beam's power, L is the traveled distance in the medium, and A is the cross-sectional area. Laser beam has a finite cross section. However, due to SPM, laser beam will appear to have self-diffraction, which is responsible for the known nonlinear optical phenomena of self-focusing and self-defocusing. Moreover, the temporal variation of the laser intensity leads to SPM in time. As the time derivative of the phase of a wave is simply the angular frequency of the wave, SPM also appears as frequency modulation.

### *3.2.2 Self-focusing and self-defocusing effects*

Another attention-grabbing phenomenon of light-matter interaction associated with SPM is self-focusing. It occurs whenever the strong field of a laser beam propagates in a third-order nonlinear medium whose refractive index depends on the beam intensity. The real part of the third-order susceptibility results in a change in the index of refraction of the material [7].

If the nonlinear refractive index is positive and the incident beam is of higher intensity in the center than the edge, then self-focusing will occur. In that case, the refractive index and the optical path length for rays at the center are greater than those at their edges. The same condition will occur for propagation via focusing lens and, because of that, the light beam will create its own positive lens in the nonlinear medium. Furthermore, when the beam focusing increases, the strength of the nonlinear lens increases resulting in stronger focusing and strength of the lens, this will result in catastrophic focusing where the beam is breaking down into a very intense small spot. This phenomenon may occur in materials that have transparency at high intensity such as crystals, glasses, gases, liquids, and plasmas [8].

In contrast, if the nonlinear refractive index is negative and the incident beam is of higher intensity in the center than the edge, then self-defocusing will occur. In that case, the refractive index and the short optical path length for rays at the center are smaller than those at their edges. The same condition will occur for propagation via negative focal length lens and beam defocuses [7].

### *3.2.3 Two-photon absorption (TPA)*

Two-photon absorption is a nonlinear absorption process where two photons of identical or different frequencies are simultaneously absorbed when an intense

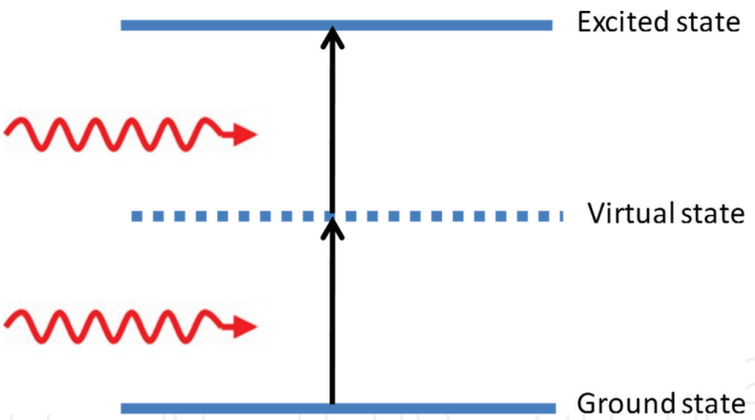



**Figure 5.**
*Schematic illustration of two-photon absorption process.*

coherent beam propagates in a third-order nonlinear medium as illustrated in **Figure 5** [11].

### 3.3 Optical limiting (OL)

Optical limiter is a device that exhibits a linear transmittance to power, irradiance, energy, or fluence below a threshold and clamps the output to a constant above it as shown in **Figure 6** [5, 11, 12], thereby providing safety to sensors or eyes because nonlinear absorption coefficient increases with increase in input power. Increase of sample temperature due to absorption results in nonlinear absorption coefficient and optical limiting effect [13]. To behave as an active optical limiter, the nonlinear optical medium must possesses high linear transmittance, low limiting threshold, fast response time, broadband response, and low optical scattering [14].

Researches on optical limiting (OL) effect started in the 1960s by Geusic et al and Ralston et al. with three-photon nonlinear absorption in inorganic semiconductors. Many demonstrations of optimized OL effect were accomplished through two-photon absorption (TPA) followed by subsequent excited state absorption (ESA).

Besides the effect of nonlinear refraction, nonlinear absorption is another kind of mechanisms used in OL. Reverse saturable absorption RSA and TPA are nonlinear absorption mechanisms used in OL [15, 16]. TPA-based devices are also proper for other applications such as optical power stabilization, optical pulse reshaping, and optical spatial field reshaping [5, 17]. Combining nonlinear

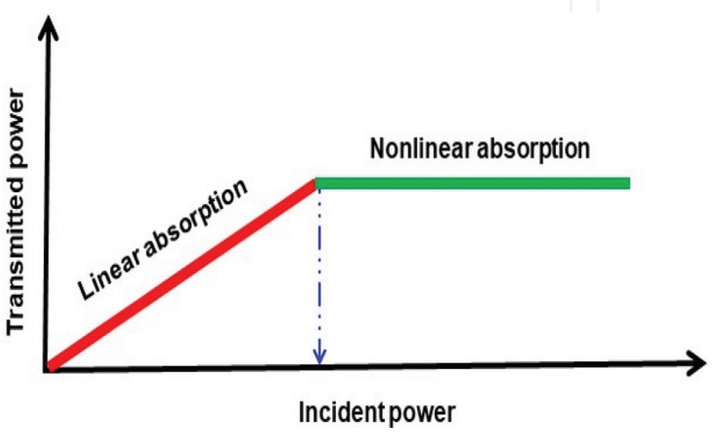



**Figure 6.**
*Optical response of an optical limiter to incident power.*

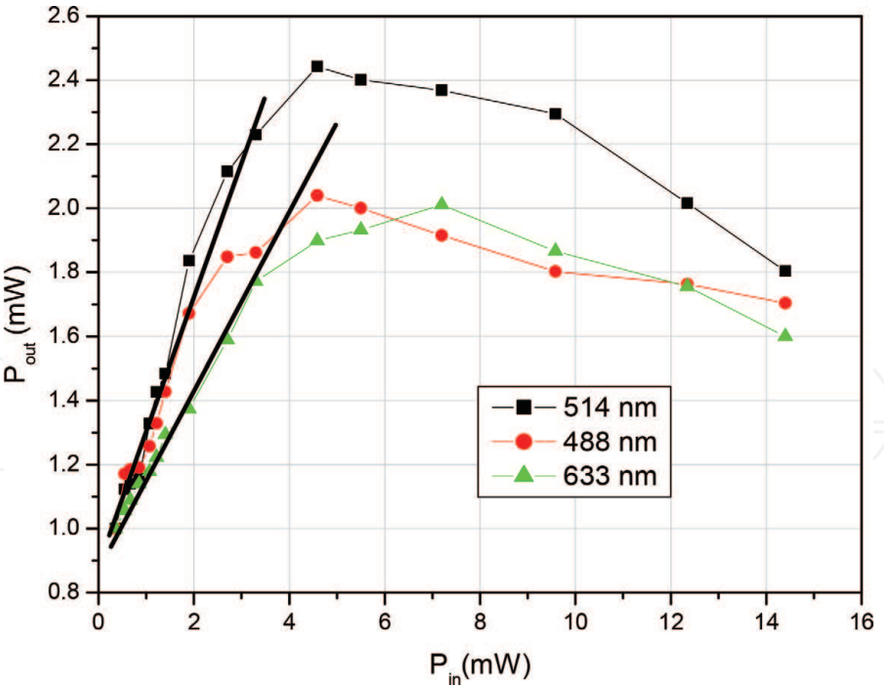



**Figure 7.**
*Optical limiting response of PbS QDs of radius 5.0 nm excited at different wavelengths.*

mechanisms has as well accomplished improvement in optical limiting, such as self-defocusing with TPA, TPA with excited state absorption (ESA). Inorganic materials combine ESA and RSA [12]. **Figure 7** shows optical limiting effect by PbS QDs of radius 5.0 nm excited with continuous wave (CW) Ar ion laser ($\lambda$ = 488 and 514 nm) and HeNe laser ($\lambda$ = 633 nm). It is obvious from **Figure 7** that OL threshold is wavelength dependent.

## 4. Characterization techniques

Many experimental techniques have been developed in order to achieve precise measurement of both nonlinear absorption coefficient ($\beta$) and nonlinear index of refraction coefficient ($n_2$) and then calculating the third-order susceptibility $\chi^{(3)}$. Examples of techniques that are in use are: nonlinear interferometry, degenerate four-wave mixing (DFWM), nearly degenerate three-wave mixing, ellipse rotation, and beam distortion measurements. However, a simple, and quite very accurate technique named Z-scan technique is widely in use and trusted (by majority of nonlinear optics researchers) to measure and tell the sign of both $\beta$ and $n_2$, and hence calculating magnitude of $\chi^{(3)}$ [18–20]. Z-scan technique is a well-established technique in characterizing third-order nonlinearity mainly because it is experimentally easy to construct and optimized. The nature and sign of nonlinearity can be identified from the raw data. These data do not require elaborated mathematical analysis.

The main idea of the Z-scan technique is to measure the intensity change in incident Gaussian laser beam transmission intensity through the sample as a function of its position (Z-position) from the focus of the beam. Transmitted beam is collected by means of two detector arrangements: closed aperture (CA) in order to recognize the sign and measure $n_2$ as illustrated in **Figure 8**, and open aperture (OA) in order to measure $\beta$. The working principle of Z-scan technique is based on the motion of the sample along the so-called Z axis from –Z to +Z through the focus

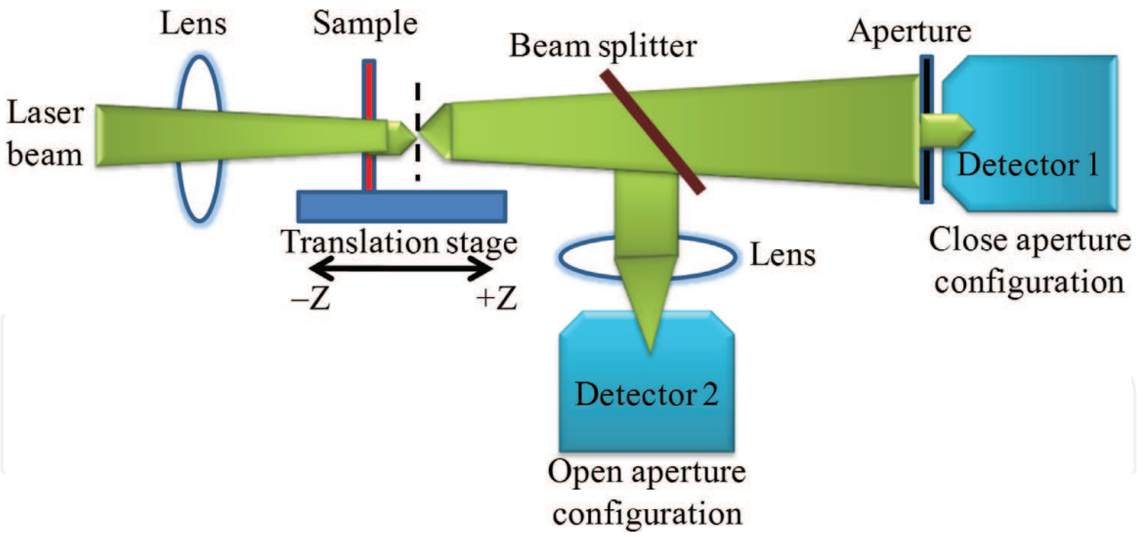



**Figure 8.**
*Schematics of experimental setup used for the closed- and open-aperture Z-scan.*

of a tightly focused Gaussian laser beam. The motion of the sample across the focused beam exposes it to a varying irradiance (intensity) level reaching its maximum value at the focus point as shown in **Figure 8**.

In this chapter, in order to apply theoretical models developed by Mansoor Sheik Bahae [18–20], samples must be prepared in the form of thin samples. A thin sample is an optical medium with thickness smaller than the diffraction length of a focused Gaussian beam.

### 4.1 Closed-aperture Z-scan configuration

As shown in **Figure 8**, if a thin sample is scanned with closed-aperture setup and Gaussian laser beam, both the sign and magnitude of nonlinear refractive index are determined. Considering a sample with negative nonlinear refractive index (self-defocusing), the scan starts far from focal length (–Z) and the sample exhibits negligible nonlinear refraction at low irradiance. As the sample gets closer to the focus beam, irradiance increases, and the sample starts acting as a negative lens. The transmittance through the aperture changes because of variation of sample location relative to the focus. When the sample becomes very close to the focus, it starts acting as a negative lens, and hence, the beam irradiance arriving at the aperture increases due to self-defocusing behavior. Conversely, as the sample moves away from the focus (+Z), the beam irradiance arriving at the detector decreases due to self-focusing effect. The transmittance becomes linear again when the scan ends. The result of this scan is represented in the transmittance versus position curve as shown in **Figure 9a**. A material possessing negative nonlinear refractive index (self-defocusing behavior) gives a transmittance with peak followed by a valley. However, sample with positive nonlinear index of refraction (self-focusing behavior) shows transmittance with valley followed by a peak as shown in **Figure 9b**. Thus, the sign of a material's nonlinearity can be determined directly from the transmittance versus position curve. This is a special feature of the Z-scan technique.

Although CA configuration is sensitive to nonlinear index of refraction, presence of nonlinear absorption can be detected on the transmittance curve. The presence of two-photon absorption (TPA) or reverse saturable absorption (RSA) enhances the valley and suppresses the peak as presented in **Figure 10a**. On the other hand, the presence of nonlinear absorption effect due to saturable absorption (SA) enhances the peak and suppresses the valley as shown in **Figure 10b** [18].

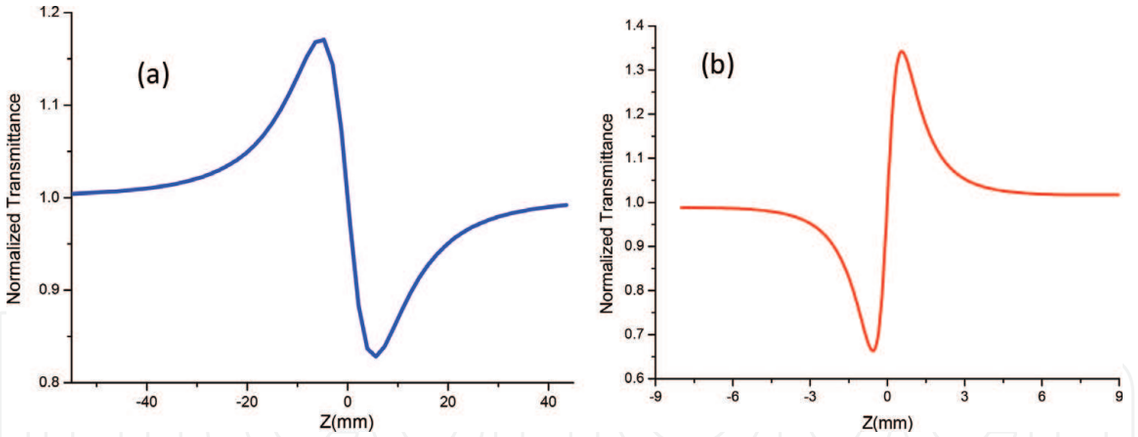



**Figure 9.**
*Closed-aperture Z-scan normalized transmittance curve: (a) negative $n_2$, and (b) positive $n_2$.*

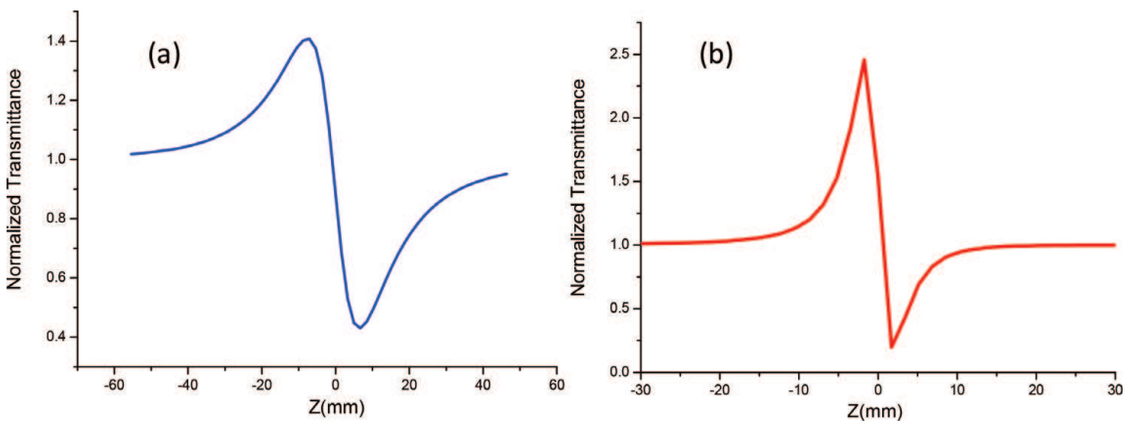



**Figure 10.**
*Closed- aperture Z-scan effect of nonlinear absorption on transmittance of the sample in the presence of: (a) two photon absorption or reverse saturable absorption, and (b) saturable absorption.*

## 4.2 Open-aperture Z-scan

When Z-scan is performed with open-aperture configuration by removing the aperture in front of the detector D2 shown in **Figure 8**, the nonlinear absorption coefficient is calculated from the normalized transmittance curve. Sample transmittance decreases (increases) as sample position Z gets closer to the focus point of the lens with minimum (maximum) value of the transmittance at the focal point, then it increases (decreases) as the sample moves away from the focus and reaches its linear behavior at far +Z position as illustrated in **Figure 11**.

In **Figure 11**, transmittance versus position curve has a symmetric shape around the focus; this is due to the symmetry of the Gaussian beam irradiance. If the transmittance is minimum at the focus (valley) as shown in **Figure 11**, this indicates the existence of two-photon absorption (TAP) or RSA with a positive type of nonlinear absorption. However, when the transmittance is maximum at the focus (peak), this indicates the presence of saturable absorption (SA) with negative type of nonlinear absorption [7, 11].

Z-scan technique requires a high-quality Gaussian beam for measurement. Tilting of sample during the scan affects the outcome of the scan. Also, the Z-scan technique is sensitive to all nonlinear optical mechanisms that give rise to a change of the refractive index and/or absorption coefficient. Thus, it is not possible to find out the original physical processes obtained from Z-scan technique.

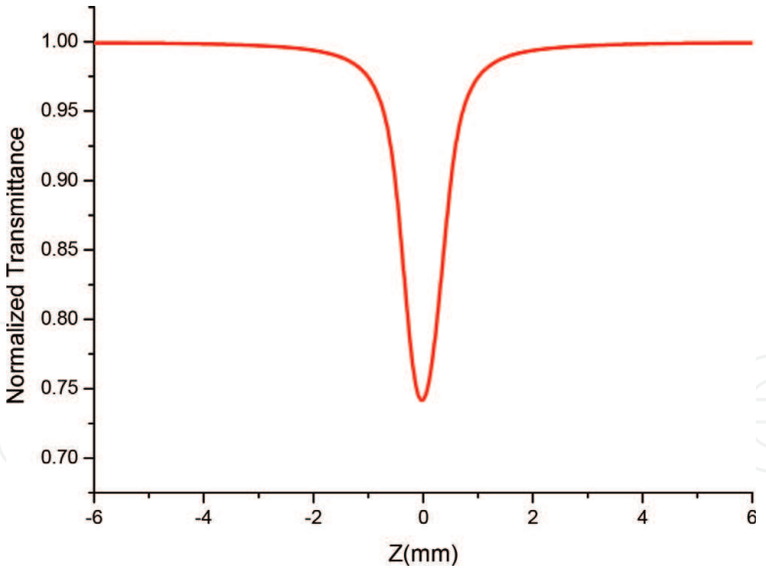



**Figure 11.**
*Open-aperture Z-scan normalized transmittance curve.*

### 4.3 Theoretical analysis

In nonlinear media, as a result of absorption of high-intensity excitation beam, the temperature in the surface of the sample exhibits a spatial distribution that creates a spatial variation of the refractive index that produces a thermal lens and hence a phase distortion of the propagating laser beam is produced. The normalized peak-to-valley transmittance $\Delta T_{pv}$ is linearly related to the phase distortion $\Delta\Phi_o$ through the following [21]:

$$\Delta T_{PV} = A\,\Delta\Phi_0 \tag{11}$$

where A is a constant given by:

$$\mathrm{A} = 0.406\,(1\text{-S})^{0.25} \tag{12}$$

$$S = 1 - \exp\left(-2r_a^2/\omega_a^2\right) \tag{13}$$

where $S$ is the aperture linear transmittance, $r_a$ is the aperture radius, and $\omega_a$ is the beam spot size (radius) at the aperture. The phase distortion $\Delta\Phi_0$ is defined as

$$\Delta\Phi_0 = k n_2 I_o L_{eff} \tag{14}$$

$$I_o = 2P_o/\pi\omega_o^2 \tag{15}$$

where $I_o$ is the intensity of the laser beam at the focus (z = 0), $P_o$ is the instantaneous input laser power into the sample, k= 2π/λ is the wave number, $n_2$ is the nonlinear refractive index, and $L_{eff}$ is the effective thickness of the sample,

$$L_{eff} = [1 - \exp(-\alpha_o L)]/\alpha_o \tag{16}$$

where $\alpha_0$ is the linear absorption coefficient and $L$ is the thickness of the sample. The nonlinear absorption coefficient β is given by [22]

$$\beta = \frac{2\sqrt{2}T_{\min}}{I_o L_{eff}} \tag{17}$$

where $T_{min}$ is the normalized transmittance of the open aperture.

The third-order nonlinear optical susceptibility $\chi^{(3)}$ can be calculated once the nonlinear refractive index $n_2$ and the nonlinear absorption coefficient $\beta$ are known using Eqs. 7–9 . The suitability of the material for all-optical switching can be evaluated using the figure of merit [23]:

$$W = n_2 I/\alpha_0 \lambda \tag{18}$$

The values W >> 1 are ideal for applications in all-optical switching.

In many situations, absorption and nonlinear index are mixed together (as shown in **Figure 10**). Consequently, one needs to adopt the Gaussian decomposition (GD) method, which was implemented by Sheik-Bahae and his co-workers [18–20]. This method consists of some complex mathematical steps to decompose the complex electric field emerging from the sample into a summation of Gaussian beams through Taylor series expansion of the nonlinear phase term. Since only small phase changes are considered, few terms of Taylor expansions are used. The normalized Z-scan transmittance T(z) can be calculated by using the following equation:

$$T(z) = \frac{\int_{-\infty}^{+\infty} P_T(z, \Delta\phi_0(t))dt}{S\int_{-\infty}^{+\infty} P_0(t)dt} \tag{19}$$

where $P_T$ (z,$\Delta\phi_0$(t)) is the transmitted power through the aperture, $P_0$(t) (Eq. 15) is the instantaneous input power (within the sample), and S is linear transmittance through the aperture. T(z) does not depend on the geometry or the wavelength while the size of aperture is an effective parameter. In case of large aperture (S = 1) the effect will disappear in T(z) in all z and $\Delta\phi_0$.

In some cases, material nonlinear absorption is weak and nonlinear refraction is more pronounced such that the transmittance curve obtained in closed-aperture configuration shows symmetric peak and valley. Therefore, one can fit the normalized transmittance curves to calculate the nonlinear index of refraction using the following equation:

$$T(z) = 1 + \frac{4x\Delta\phi_0}{(x^2+9)(x^2+1)} \tag{20}$$

where x = z/$z_R$, $z_R = \pi\omega_0^2/\lambda$ is the Rayleigh range or the diffraction length of the Gaussian beam, $\omega_0$ is the beam's waist, and $\Delta\phi_0$ is the on-axis phase shift due to nonlinear refraction expressed as:

$$\Delta\phi_0 = kn_2 I_0 L_{eff} \tag{21}$$

Nonlinear absorption coefficient β can be calculated by fitting the open-aperture normalized transmittance curve using the following equation:

$$T(z) = 1 - \frac{\Delta\Psi_0}{(x^2+1)} \tag{22}$$

where $\Delta\Psi_0$ is the on-axis phase shift due to nonlinear absorption expressed as:

$$\Delta\Psi_0 = \frac{I_0 L_{eff}}{2\sqrt{2}}\beta \tag{23}$$

In many situations, both nonlinear refraction and nonlinear absorption are mixed such that the closed-aperture transmittance shows asymmetric peak-valley curve like the one presented in **Figure 10**. In this case, the normalized transmittance curves are fitted using the following equation [15]:

$$T(z) = 1 + \frac{4x\Delta\phi_0}{(x^2+9)(x^2+1)} - \frac{2(x^2+3)\Delta\Psi_0}{(x^2+9)(x^2+1)} \tag{24}$$

The nonlinear refractive index and nonlinear absorption coefficient are calculated from Eqs. (21) and (23).

In cases of high single-photon absorption using CW laser even at few mill watts, thermal lensing becomes pronounced such that the Gaussian decomposition model will not be suitable to fit data since the closed-aperture normalized transmittance shows a very slow return to the normal transmittance as the sample is scanned further away from focal point (+Z) (for example see **Figure 12**). Therefore, a modified model has been suggested by [24], called the thermal-lens model. The normalized transmission of closed-aperture Z-scan is given by:

$$T(z) = \left(1 + \Delta\phi_0 \frac{2x}{(x^2+1)} + \Delta\phi_0^2 \frac{2x}{(x^2+1)}\right)^{-1} \tag{25}$$

**Figure 12** shows the importance of adopting thermal model to get proper fitting of the collected data.

However, as shown in **Figure 13**, thermal lens model fails to fit properly the closed-aperture normalized transmittance data for the same PbS quantum dots (radius 2.4 nm) when excitation power $P_0$ = 6 mW but wavelength is 633 nm. Application of the Gaussian decomposition model resulted in better fitting of data. In conclusion, the investigator in order to accurately calculate third-order nonlinear parameters must chose the most proper fitting model.

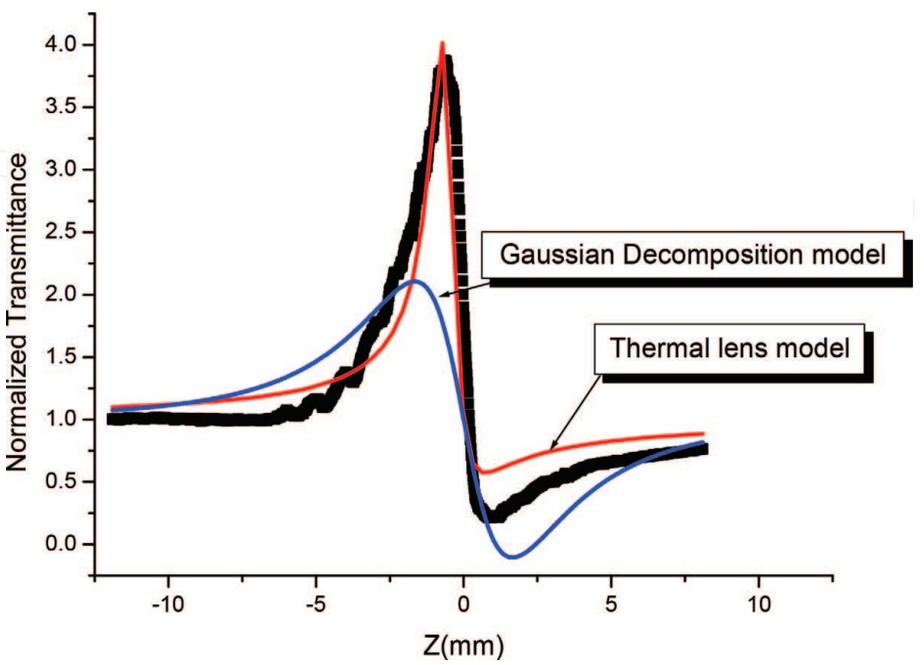



**Figure 12.**
*Closed-aperture Z-scan effect of PdS quantum dots (radius 2.4 nm) irradiated with laser beam (λ = 488 nm and $P_o$ = 6 mW); the data points ( black) are fitted with the thermal lens model (red curve) and Gaussian decomposition model (blue curve).*

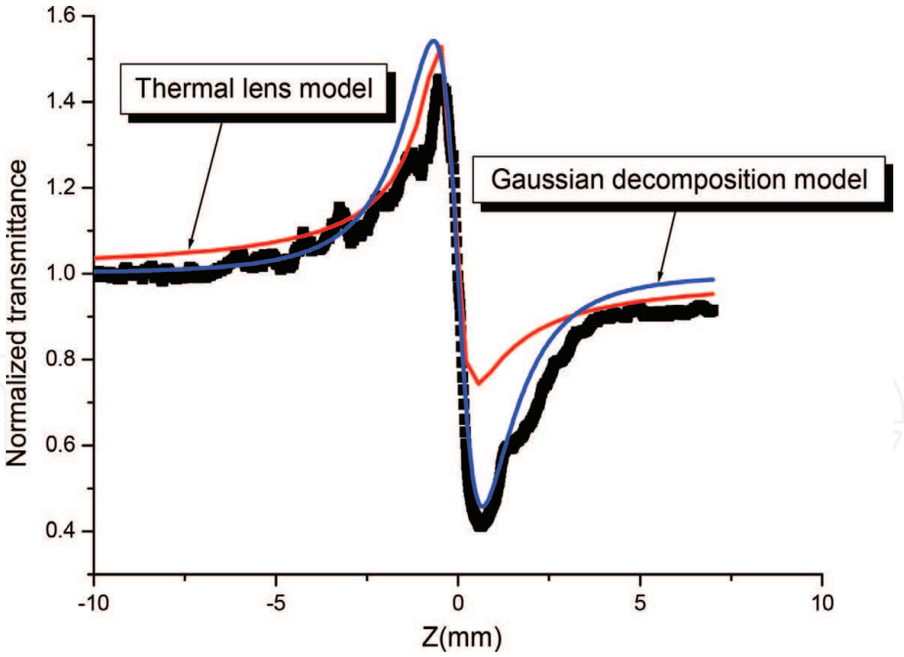



**Figure 13.**
*Closed-aperture Z-scan effect of PdS quantum dots (radius 2.4 nm) irradiated with laser beam ($\lambda$ = 633 nm and $P_o$ = 6 mW); the data points (black) are fitted with the thermal lens model (red curve) and Gaussian decomposition model (blue curve).*

## 5. Characterization of PbS QDs suspended in toluene

In this section, we will present—as an example—some nonlinear optical findings for samples of lead sulfide (PbS) quantum dots suspended in toluene. One sample of QDs has an average size (radius) of 2.4 nm and the other is with size 5.0 nm. It is very important to ensure that the sample is not contaminated with any impurities during QDs synthesis and storing or handling. The purity of the toluene quantum dot system was verified by NMR measurements where a small amount of the QD solution is dissolved in deuterated chloroform ($CdCl_3$). Therefore, any hydrogen in the solvent gets replaced by deuterium and only hydrogen will be originating from toluene. As shown in **Figure 14**, the peak at 0.00 ppm is for the TMS reference. The only peaks that appear are those by toluene that reveal the absence of any contamination that may influence both linear and nonlinear optical properties [25].

The samples were Z-scanned in both configurations OA and CA. Example of obtained results for QDs with radius 2.4 nm at three different excitation wavelengths with beam average power of 12 mW is shown in **Figure 15**. Similar general behavior is obtained with 5.0-nm QDs. **Figure 15** indicates clearly the dependence of third-order nonlinearity on excitation wavelength.

**Figure 16** shows the closed-aperture Z-scan normalized transmittance for excitation wavelength of 633 nm, and 8-mW laser power for both the 2.4-nm and 5.0-nm QD radii. Similar transmittance curves are obtained for 488-nm and 514-nm laser excitation wavelengths. It is obvious from **Figure 16** that QD's size is a factor to be considered when quantifying third-order nonlinearity. The asymmetric curve is clearly indicative of nonlinear absorption, and the closed-aperture transmittance is affected by both nonlinear absorption and refraction. The suppression of the valley and enhancement of the peak of the transmittance curve imply that saturable absorption (SA) is the origin of nonlinear absorption effect. Whenever the excitation energy is much more than the optical bandgap or the excitation wavelength is near the peak of the absorption, saturable absorption becomes prominent due to high optical density.

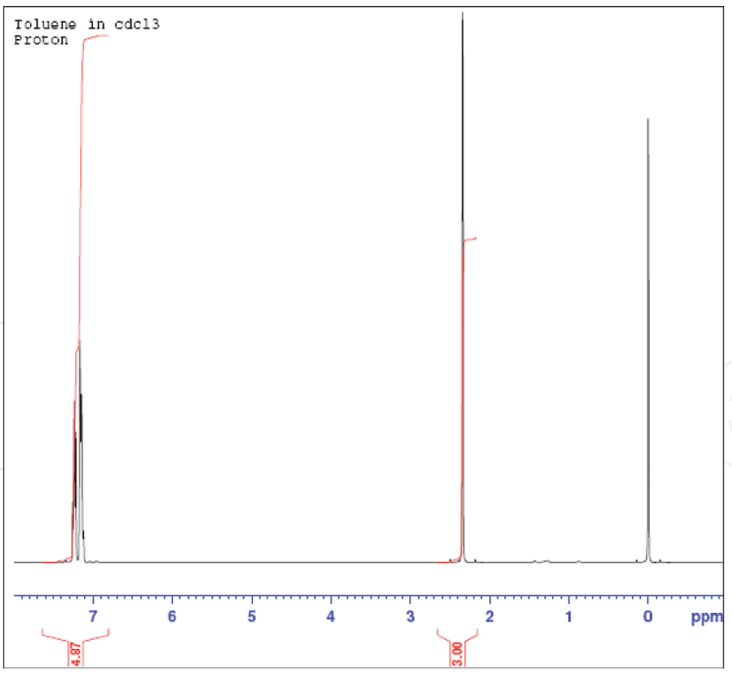



**Figure 14.**
*NMR spectrum for sample of PbS QDs suspended in toluene [25].*

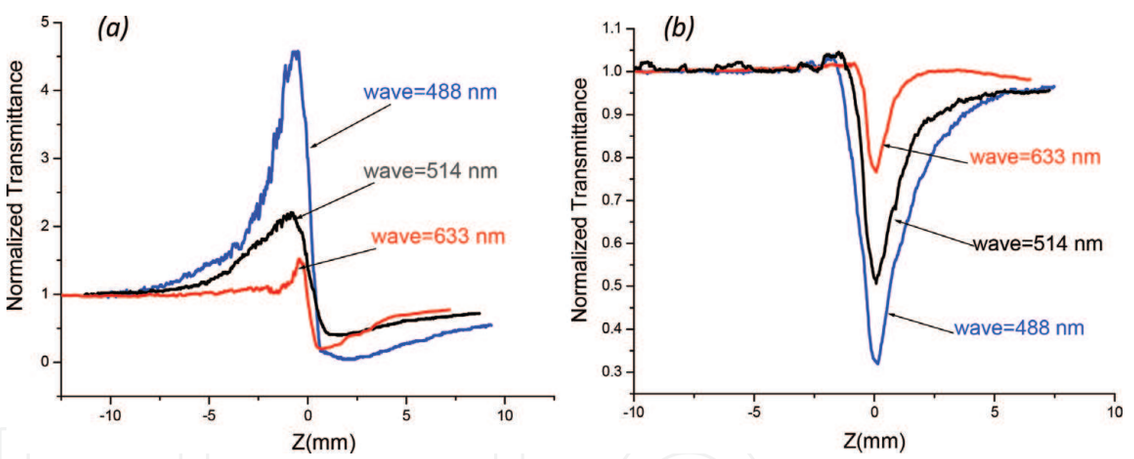



**Figure 15.**
*Obtained normalized transmittances for QDs of radius 2.4 nm excited with laser beam power of 12 mW at three different wavelengths: (a) closed aperture configuration, and (b) open aperture configuration.*

From **Figure 17**, we can not only tell the sign of the nonlinear refractive index (peak-valley = negative index) but also the origin of nonlinear refraction. Since CW lasers were used to investigate optical nonlinearity of samples, nonlinear refraction is due to thermal lensing which is a consequence of high linear absorption. Thermal lens model (solid line) was used to fit the data as presented in **Figure 17**. Moreover, it was suggested [16–19] that when the closed-aperture transmittance $\Delta T_{PV} > 1.7$, nonlinearity is due to thermal effect governing the nonlinear refraction behavior. This is clear in **Figure 17** where $\Delta T_{PV} \approx 4.5$.

**Table 2** presents the calculated nonlinear refractive index $n_2$ for two different sizes of QDs excited with beam power of 8 mW, $n_2$ increases systematically with QD's sizes and the excitation wavelength. The variation of $n_2$ value with QDs size is illustrated in **Figure 18**. There is a clear trend of increase of $n_2$ with QD size for all wavelengths used.

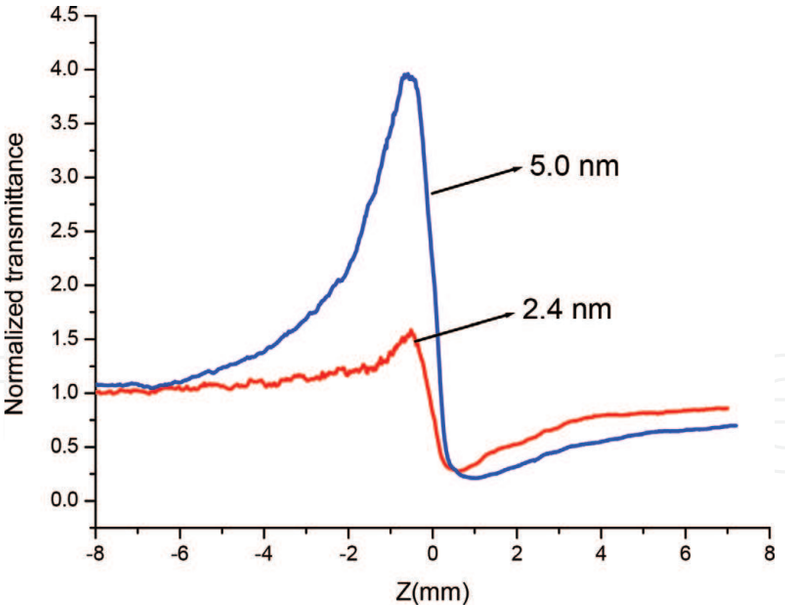



**Figure 16.**
*Closed-aperture measurements for QDs with radius 2.4 nm and 5.0 nm samples scanned with beam of $P_{in}$ = 8 mW and λ = 633 nm.*

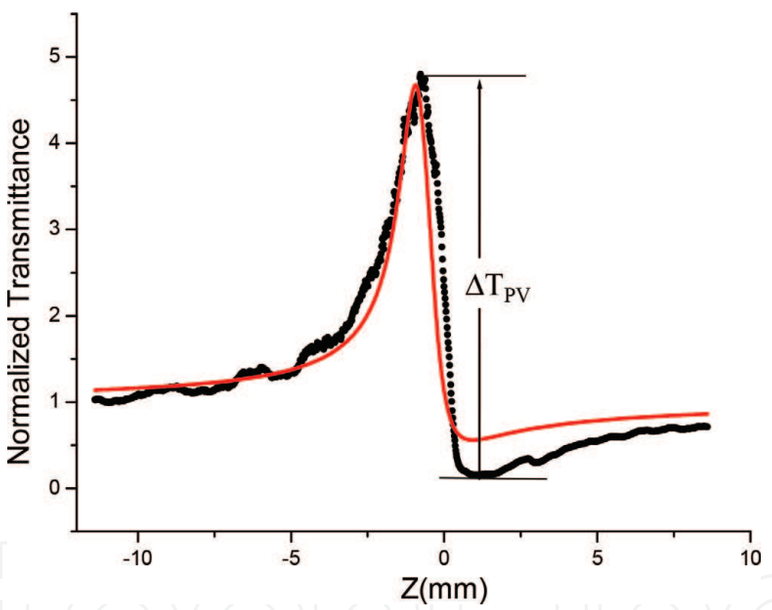



**Figure 17.**
*Fitted closed-aperture measurements for 5-nm QD size samples scanned with beam of $P_{in}$ = 8 mW and λ = 488 nm.*

| Quantum dot size (nm) | $n_2 \times 10^{-11}$ m²/W (λ = 488 nm) | $n_2 \times 10^{-11}$ m²/W (λ = 514 nm) | $n_2 \times 10^{-11}$ m²/W (λ = 633 nm) |
|---|---|---|---|
| 2.4 | 3.501 | 3.742 | 4.631 |
| 5 | 5.383 | 6.975 | 8.406 |

**Table 2.**
*Nonlinear index of refraction at different excitation wavelengths ($P_{in}$ = 8 mW).*

The nonlinear absorption coefficient β can be calculated from Eq. (17). $T_{\min}$ in this equation is obtained from the normalized open-aperture transmittance, as shown in **Figure 19**.

**Table 3** shows the nonlinear absorption coefficient at different excitation wavelengths. For a given QD radius, there is a slight increase of the nonlinear absorption

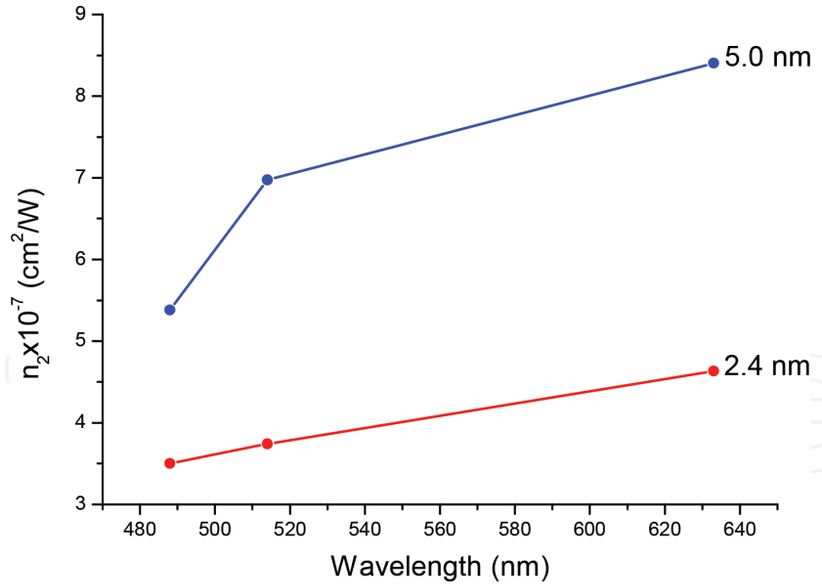



**Figure 18.**
*Nonlinear index of refraction versus excitation wavelength ($P_{in}$ = 8 mW) for different sizes of quantum dots.*

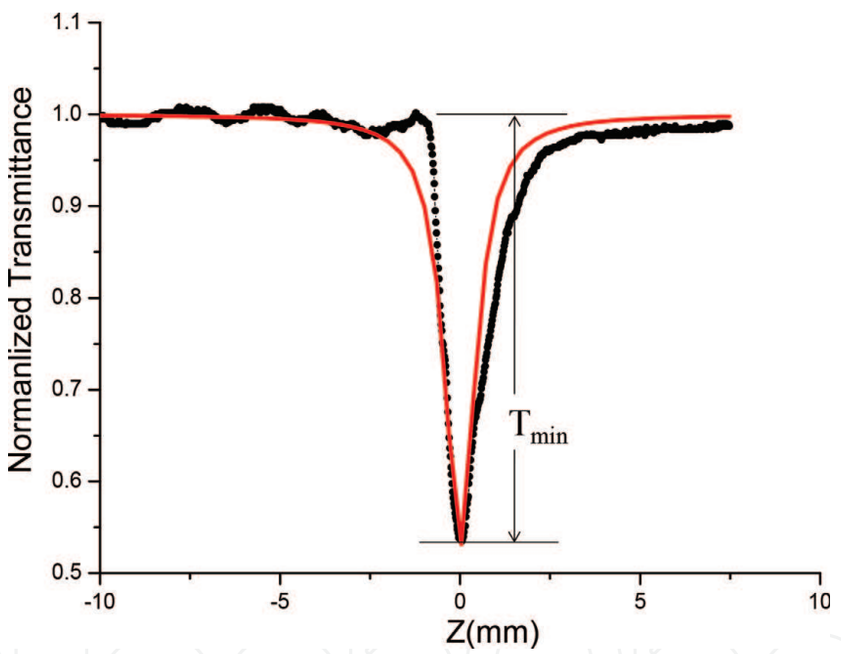



**Figure 19.**
*Fitted open-aperture measurements for 5 nm QD size sample scanned with a beam of $P_{in}$ = 8 mW and λ = 488 nm.*

| Quantum dot size (nm) | β × $10^{-5}$ m/W (λ = 488 nm) | β × $10^{-5}$ m/W (λ = 514 nm) | β × $10^{-5}$ m/W (λ = 633 nm) |
|---|---|---|---|
| 2.4 | 8.676 | 17.12 | 21.530 |
| 5.0 | **9.844** | **10.750** | **21.600** |

**Table 3.**
*Nonlinear absorption coefficient β at different excitation wavelengths ($P_{in}$ = 8 mW).*

coefficient with increasing wavelength. However, the change of the nonlinear absorption coefficient with size of QD is small.

Generally, the closed-aperture transmittance is affected by both the nonlinear refraction and nonlinear absorption. Therefore, the determination of $n_2$ is not very accurate from the closed-aperture scans alone. To obtain purely effective nonlinear

refraction, we divide the normalized closed-aperture transmittance by the corresponding open-aperture scan. Then from proper fitting model (Eq. 24) of data, one can determine both nonlinear index of refraction and nonlinear absorption coefficients.

To calculate the third-order nonlinear susceptibility, the values of $n_2$ and $\beta$ are first calculated, and then substituted in Eqns. (19) and (20). **Table 3** shows the calculated real and imaginary parts of the third-order nonlinear optical susceptibility $\chi^{(3)}$ and its absolute value $|\chi^{(3)}|$ for different values of $n_2$ and $\beta$. Investigating Eqs. (9) and (10), we observe that $\mathrm{Re}\chi^{(3)}$ is proportional to $n_2$, and $\mathrm{Im}\chi^{(3)}$ is proportional to $\beta$ for a given excitation wavelength. This is the trend of variation we observe for both the real and imaginary parts of $\chi^{(3)}$.The figure of merit W (see Eq. 18) for different QD sizes is shown in the last column of **Table 4**. For small one-photon absorption $\alpha_0$ in the near infrared region, the values W >>1 are ideal for applications in all-optical switching.

**Table 5** presents the absolute value of the third-order nonlinear susceptibility $|\chi^{(3)}|$ for excitation wavelengths of 488 nm, 514.5 nm, and 632.8 nm at a constant laser beam power of 8 mW. Even though the real and imaginary parts of $\chi^{(3)}$ show no specific trend of variation with particle size, the absolute value $|\chi^{(3)}|$ increases systematically with particle size for the three wavelengths used in our Z-scan experiments. But, for the same QD size, it seems that $|\chi^{(3)}|$ is faintly enhanced as wavelength increases.

In fact, QDs act as excellent optical limiters, an example is presented in **Figure 7**. In order to study the optical limiting behavior of a sample using the Z-scan setup, one must place the sample in the post focal position and collect the transmitted light beam by closed-aperture configuration as illustrated in **Figure 20**.

Formation of diffraction fringes is presented in **Figure 21** for excitation power levels higher than 1 mW. Also, self-fanning dominates the transmittance spectrum. From the number of these fringes, one can estimate the change in the refractive index. Such interesting behavior ranks QDs media as very attractive active part of all optical switching devices.

In the above presented results, continuous-wave laser has been used and has resulted in thermally generated third-order nonlinearity due to deposition of heat. However, one way to overcome such effect is to use pulsed laser where electronic nonlinearity gets revealed. Moreover, one must avoid high power levels of

| QD size (nm) | $n_2\times10^{-7}$ ($cm^2$/W) | $\beta\times10^{-3}$ (cm/W) | Re $\chi^{(3)}\times10^{-5}$ (esu) | Im $\chi^{(3)}\times10^{-6}$ (esu) | $\lvert\chi^{(3)}\rvert\times10^{-5}$ (esu) | W |
|---|---|---|---|---|---|---|
| *2.4* | ***3.501*** | ***8.676*** | ***2.025*** | **1.949** | **2.034** | **4.345** |
| *5.0* | ***5.389*** | ***9.844*** | ***3.116*** | **2.211** | **3.124** | **3.807** |

**Table 4.**
*Real and Imaginary parts of the third order nonlinear optical susceptibility for different QD sizes ($\lambda$ = 488 nm, $P_{in}$ = 8 mW).*

| QD size (nm) | $\lvert\chi^{(3)}\rvert\times10^{-5}$ (esu), $\lambda$ = 488 nm, P = 8 mW | $\lvert\chi^{(3)}\rvert\times10^{-5}$ (esu), $\lambda$ = 514.5 nm, P = 8 mW | $\lvert\chi^{(3)}\rvert\times10^{-5}$ (esu), $\lambda$ = 632.8 nm, P = 8 mW |
|---|---|---|---|
| 2.4 | 2.034 | 2.202 | 2.750 |
| 5.0 | 3.124 | 4.042 | 4.902 |

**Table 5.**
*The absolute value of the third-order nonlinear optical susceptibility for different QD sizes.*

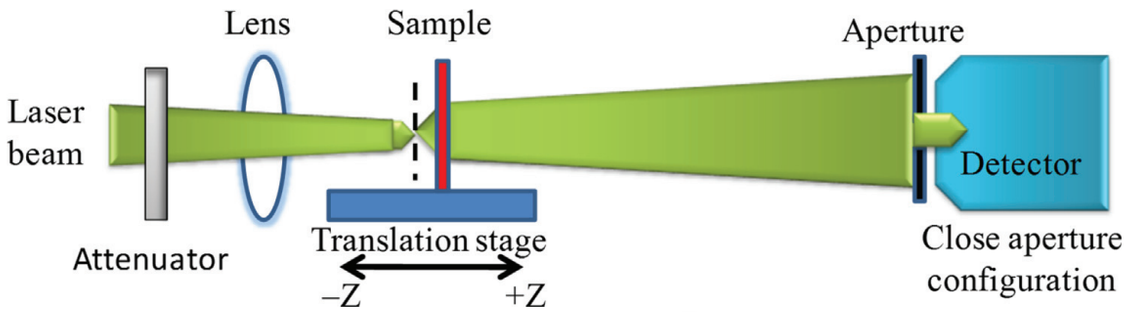



**Figure 20.**
*Schematic of optical limiting investigation setup.*

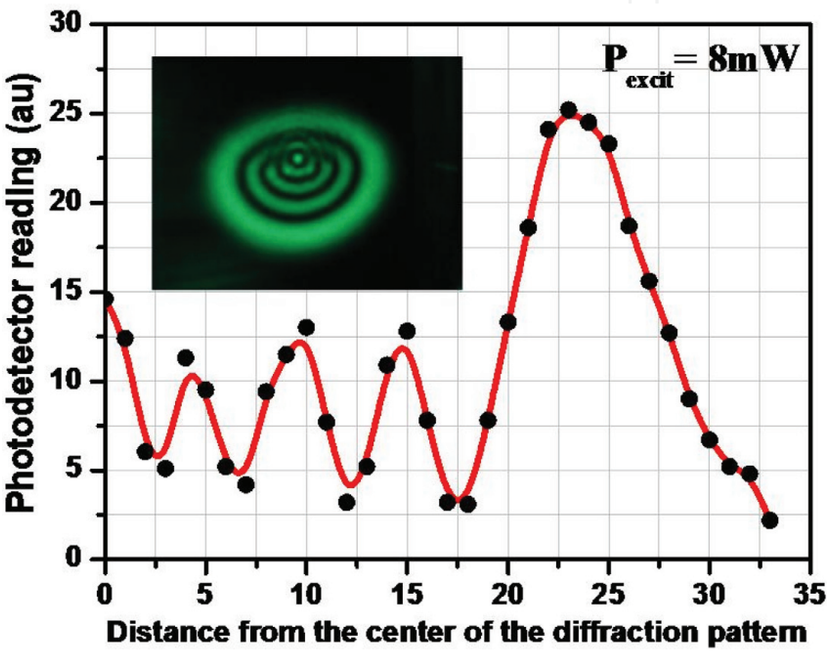



**Figure 21.**
*A photograph of the diffraction rings due to nonlinear diffraction by QD sample of 2.4-nm radius Z-scanned with $Ar^+$ laser beam (P = 8 mW, and λ = 514 nm). The dots are the photodiode reading across the rings starting from the center of the diffraction pattern, the distance is in unit of mm [25].*

excitation in order not excite higher orders of nonlinearity such as $\chi^{(5)}$ or exceeding the threshold damage of samples.

## 6. Conclusions

Quantum dots are interesting nanostructured materials. QDs are becoming an active part in many photonic devices. QDs possess unique optical and electronic properties. QD bandgap absorption edge is size dependent; as QD size is reduced, its bandgap energy gets larger. QDs possess large values of third-order nonlinear optical parameters such as nonlinear index of refraction $n_2$, nonlinear absorption coefficient β, and nonlinear susceptibility $\chi^{(3)}$. There are well-established models to explain and calculate third-order nonlinearity parameters obtained using different experimental techniques. Z-scan is considered an easy and practical technique used to investigate third-order nonlinearity for many classes of nonlinear media, among them are QDs. QD size, excitation wavelength, and incident power value are factors that need to be considered when investigating third-order nonlinearity. To separate

electronic from thermal effects on quantified nonlinearity, one must use pulsed laser rather than continuous wave (CW). QD media are excellent active parts of optical limiters and all-optical switching devices.

## Acknowledgements

The author would like to acknowledge the financial support provided by the University of Bahrain. Special thanks go to Professor Shawqi Al Dallal and Dr. Feryad Henari for their support and fruitful discussions.

IntechOpen

IntechOpen

## Author details

Khalil Ebrahim Jasim
Department of Physics, University of Bahrain, Kingdom of Bahrain

*Address all correspondence to: kejasim@uob.edu.bh

IntechOpen

© 2019 The Author(s). Licensee IntechOpen. This chapter is distributed under the terms of the Creative Commons Attribution License (http://creativecommons.org/licenses/by/3.0), which permits unrestricted use, distribution, and reproduction in any medium, provided the original work is properly cited. CC BY

## References

[1] Jasim KE. Quantum dots solar cells. In: Kosyachenko LA, editor. Solar Cells —New Approaches and Reviews. InTech Open Access Publisher; 2015. pp. 303-331. DOI: 10.5772/59159. Chapter 11

[2] Brus LE. Electronic wavefunctions in semiconductor clusters. Journal of Physical Chemistry A. 1986;**90**: 2555-2560. DOI: 10.1021/j100403a003

[3] Boyed R. Nonlinear Optics. 3rd ed. Orlando: Academic Press Inc.; 2008. ISBN: 0123694701 9780123694706

[4] Zhao P. Ultrafast mechanisms of nonlinear refraction and two-photon photochromism [thesis]. Central Florida; 2016

[5] Rashidian M, Dorranian D. Investigation of optical limiting in nanometals. Reviews On Advanced Materials Science. 2015;**40**(12):110-126. ISSN 1605-8127

[6] Hassan QM, Al-Ahmad A, Al-Mudhaffer MF, Badran HA. Third-order optical nonlinearities and optical-limiting properties of phloxine B dye doped PMMA films investigated by Z-scan technique. Romanian Journal of Physics. 2012;**58**:962-969. ISSN 1221-146X

[7] Paul B. Investigations of nonlinear optical properties of certain organic photonic materials using Z-scan and DFWM techniques [thesis]. Cochin University of Science & Technology; 2004

[8] Saleh BEA, Teich MC. Fundamentals of Photonics. 2nd ed. John Wiley & Sons Inc.; 1991. DOI: 10.1002/0471213748. ISBN: 9780471213741

[9] Rekha RK, Ramalingam A. Nonlinear characterization and optical limiting effect of carmine dye. Indian Journal of Science and Technology. 2009;**2**(8): 29-31. ISSN: 0974-5645

[10] Sun XB, Wang XQ, Ren Q, Zhang GH, Yang HL, Feng L. Third-order nonlinear optical properties of bis (tetrabuty-lammonium)bis (4,5-dithiolato-1, 3-dithiole-2-thion) copper. Materials Research Bulletin. 2006;**41**: 177-182. DOI: 10.1016/j.materresbull.2005.07.021

[11] Pramodini S. Third order optical nonlinearity and optical power limiting of organic materials under CW laser illumination [thesis]. Manipal University; 2015

[12] Krishnamurthy R, Alkondan R. Nonlinear characterization of mercurochrome dye for potential application in optical lmiting. Optical Application. 2010;**1**:187-196. ISSN 1899-7015

[13] Rashidian M, Dorranian D, Darani SA, Saghafi S, Ghoranneviss M. Nonlinear responses and optical limiting behaviour of Basic Violet 16 dye under CW laser illumination. Optik—International Journal for Light and Electron Optics. 2009;**120**(18): 1000-1006. DOI: 10.1016/j.ijleo.2008.05.001

[14] Al-Saidi IA, Abdulkareem SA. Nonlinear optical properties and optical power limiting of Leishman dye using z-scan technique. Journal of Materials Science. Materials in Electronics. 2015; **26**(5):2713-2718. DOI: 10.1007/s10854-015-2747-3

[15] Ganeev R, Ryasnyansky A, Redkorechev V, Fostiropoulos K, Priebe G, Usmanov T. Variations of nonlinear optical characteristics of C60 thin films at 532 nm. Optics Communications. 2003;**225**(1-3):131-139. DOI: 10.1016/j.optcom.2003.07.019

[16] Rao SV, Anusha PT, Prashant TS, Swain D, Tewari SP. Ultrafast nonlinear optical and optical limiting properties of phthalocyanine thin films studied using z-scan. Materials Sciences and Applications. 2011;**02**(05):299-306. DOI: 10.4236/msa.2011.25039

[17] Zongo S. Nonlinear optical properties of natural dyes based on optical resonance [thesis]. Western Cape; 2012

[18] Sheik-Bahae M, Said A, Wei T, Hagan D, Stryland EW. Sensitive measurement of optical nonlinearities using a single beam. IEEE Journal of Quantum Electronics. 2007;**26**(4): 760-769. **ISSN:** 0018-9197

[19] Sheik-Bahae M, Said AA, Van Stryland EW. High sensitivity, single-beam $n_2$ measurement. Optics Letters. 1989;**14**:955-957. DOI: 10.1364/OL.14.000955

[20] Sheik-Bahae M, Said AA, Wei TH, Hagan DJ, Van Stryland EW. Sensitive measurement of optical nonlinearities using a single beam. IEEE Journal of Quantum Electronics. 1990;**26**:760-769. DOI: 10.1109/3.53394

[21] Mathews SJ, Chaitanya Kumar S, Giribabu L, Vengopal Rao S. Nonlinear optical and optical limiting properties of phthalocyanines in solution and thin film of PMMA at 633 nm studies using a cw laser. Materials Letters. 2007;**61**: 4426-4431. DOI: 10.1016/j.matlet.2007.02.034

[22] Vinitha G, Ramalingam A. Spectral characteristics and nonlinear studies of methyl violet 2B dye in liquid and solid media. Laser Physics. 2008;**18**:37-42. DOI: 10.1134/S1054660X08010076

[23] Hou HW, Meng XR, Song YL, Fan YT, Zhu Y, Lu HJ, et al. Two-dimensional rhombohedral grid coordination polymers [M(bbbt)2 (NCS)2]n (M = Co, Mn, or Cd; bbbt = 1,1-(1,4- butanediyl) bis-1H-benzotriazole): Synthesis, crystal structures, and third- order nonlinear optical properties. Inorganic Chemistry. 2002;**41**(15):4068-4075. DOI: 10.1134/S1054660X08010076

[24] Cuppo FLS, Neto AMF, Gömeze SL, Muhoray PP. Thermal-lens model compared with the Sheik-Bahae formalism in interpreting Z-scan experiments on lyotropic liquid crystals. Journal of the Optical Society of America B. 2002;**19**:1342-1348. DOI: 10.1364/JOSAB.19.001342

[25] Khalil Ebrahim J, Al Dallal S. Fluorescence and nonlinear optics of PbS quantum dots dispersed in toluene. Journal of Experimental Physics. 2014;**1**: 19-28. ISSN 2384-4779